

Detecting modules in quantitative bipartite networks: the QuaBiMo algorithm

Carsten F. Dormann*

Biometry and Environmental System Analysis
University of Freiburg, Germany

Rouven Strauss

Department of Computer Science
Technion - Israel Institute of Technology, Haifa, Israel

April 12, 2013

Abstract

Ecological networks are often composed of different sub-communities (often referred to as modules). Identifying such modules has the potential to develop a better understanding of the assembly of ecological communities and to investigate functional overlap or specialisation. The most informative form of networks are quantitative or weighted networks. Here we introduce an algorithm to identify modules in quantitative bipartite (or two-mode) networks. It is based on the hierarchical random graphs concept of Clauset *et al.* (2008 Nature 453: 98–101) and is extended to include quantitative information and adapted to work with bipartite graphs. We define the algorithm, which we call QuaBiMo, sketch its performance on simulated data and illustrate its potential usefulness with a case study.

1 Introduction

The ecological literature is replete with references to interacting groups of species within systems, variously termed compartments (May, 1973; Pimm, 1982; Prado & Lewinsohn, 2004), modules (Olesen *et al.*, 2007; Garcia-Domingo & Saldaña, 2008; Dupont & Olesen, 2009), cohesive groups (Bascompte *et al.*, 2003; Danieli-Silva *et al.*, 2011; Guimarães Jr *et al.*, 2011) or simply communities (Fortunato, 2010). Their attraction, for ecologists, is that they promise a way to simplify the description and understanding of an ecological system, by representing not each and every species, but aggregating their interactions and energy fluxes into a more manageable set of modules (e.g. Allesina, 2009). In the following, we will refer to such aggregated sets of interacting species as ‘modules’. Their characteristic hallmark is that *within*-module interactions are more prevalent than *between*-module interactions (Newman, 2003; Newman & Girvan, 2004; Fortunato, 2010).

In the extreme case, modules are completely separated from each another, and are then typically called compartments (Pimm, 1982). This strict definition has seen some relaxation (Dicks *et al.*, 2002), but most recent studies converge on the term module for any identifiable substructure in interaction networks (Prado & Lewinsohn, 2004; Lewinsohn *et al.*, 2006; Olesen *et al.*, 2007; Ings *et al.*, 2009; Joppa *et al.*, 2009; Cagnolo *et al.*, 2010).

The identification of modules, and the membership of species to modules, has received considerable interest in the physical sciences (as reviewed *in extenso* by Fortunato, 2010). Particularly

*Corresponding author; email: carsten.dormann@biom.uni-freiburg.de

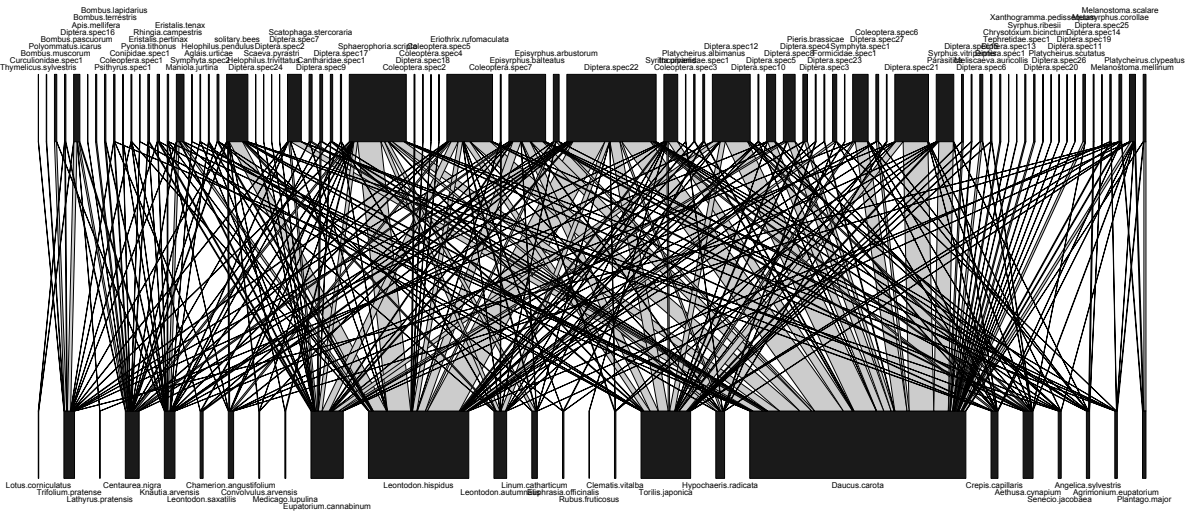


Figure 1: Bipartite graph of a quantitative pollinator-visitation network (Memmott, 1999).

29 the work of Newman and co-workers (e.g. Newman, 2003; Newman & Girvan, 2004) has practi-
 30 cally defined the current paradigm of module definition and identification. Algorithms to identify
 31 modules are “greedy”, i.e. highly computationally intensive, relying on some way of rearranging
 32 module memberships and then quantifying “modularity” until a maximal degree of sorting has
 33 been achieved (Newman, 2004; Clauset *et al.*, 2004; Newman, 2006; Schuetz & Caflich, 2008).
 34 The focus of virtually all these algorithms was on unweighted and one-mode networks (see, e.g.,
 35 Clauset *et al.*, 2008; Lancichinetti & Fortunato, 2011; Jacobi *et al.*, 2012, for a recent examples).
 36 Unweighted (or binary or qualitative) refers to the fact that only the presence of a link between
 37 species is known, but not its strength (Levins, 1975; Pimm, 1982). One-mode refers to the struc-
 38 ture of the community, in which all species are potentially interacting with each other. The typical
 39 ecological example is a $n \times n$ food web matrix, in which entries of 1 depict an existing interaction.

40 In recent years, weighted and bipartite interaction networks have become more intensively
 41 studies. In a weighted network the link between two species is actually quantified (e.g. by the
 42 number of interactions observed or the strength of the interaction inferred from the data). In a bi-
 43 partite network the species fall into two different groups, which interact with members of the other
 44 group, but not within their group. A typical example are pollinator-visitation networks (Vázquez
 45 *et al.*, 2009), where pollinators interact with flowers, but flowers do not interact among themselves
 46 (see Fig. 1). Another well-studied example are host-parasitoid networks (e.g. Morris *et al.*, 2004;
 47 Tylisanakis *et al.*, 2007) or seed dispersal networks (Schleuning *et al.*, 2012).

48 While popular among ecologists (Blüthgen, 2010; Schleuning *et al.*, 2012; Poisot *et al.*, 2012;
 49 Pocock *et al.*, 2012), weighted bipartite graphs are not amenable to any of the existing module-
 50 detection algorithms for one-mode networks or for unweighted bipartite networks. Existing soft-
 51 ware uses only one-mode networks or, more precisely, one-mode projections of bipartite networks
 52 (Guimerà *et al.*, 2007; Martín González *et al.*, 2012; Thébault, 2013), while other approaches fo-
 53 cus on the identification of crucial species through quantifications of their position in the network
 54 (Borgatti, 2006). This lack of an algorithm to identify modules in quantitative, bipartite networks
 55 is particularly problematic, as such networks find their way into conservation ecological consid-
 56 erations (Tylisanakis *et al.*, 2010) and are the focus of a vibrant field of macroecological research
 57 (Ings *et al.*, 2009). Furthermore, from a statistical point of view, weighted networks offer much
 58 more information and are less likely to lead to erroneous conclusions about the system (Barber,
 59 2007; Scotti *et al.*, 2007; Blüthgen, 2010).

60 Here we present an algorithm to identify modules (and modules within modules) in weighted
 61 bipartite networks. We build on an algorithm provided by Clauset *et al.* (2008) for unweighted,

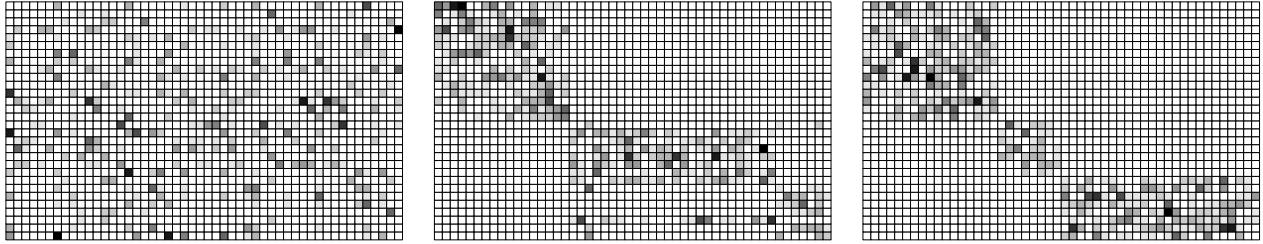


Figure 2: A simulated 3-compartment network in random sequence (left), as sorted by a correspondence analysis (centre) and by the modularity algorithm with default settings (right).

62 one-mode networks and the module criterion developed from Newman’s one-mode version by
 63 Barber (2007).

64 2 Modularity algorithms

65 Modules can be interpreted as link-rich clusters of species in a community. An alternative to
 66 finding and delimiting such modules is to group species by ordination (Lewinsohn *et al.*, 2006).
 67 Correspondence analysis (CA) of the adjacency matrix is a simple and fast way to organise
 68 species. Typically, however, correspondence analysis will not be able to identify modules suf-
 69 ficiently well, even if modules are actually compartments (i.e. perfectly separated: Fig. 2 left,
 70 centre). The QuaBiMo algorithm we present here, can do so, at least in principle (Fig. 2 right). If
 71 modules are perfectly separated, with no species interacting with species in another module, they
 72 are called compartments and will be visible as clearly separated groups of species. It is relatively
 73 straightforward to implement a recursive compartment detection function, but compartments are
 74 much coarser than modules and not the topic of this publication.

75 One algorithm proposed and available for detecting modules in bipartite networks is due to
 76 Guimerà *et al.* (2007, called “bipart_w”), which is based on an a one-mode algorithm (Guimerà
 77 *et al.*, 2005). Their approach differs substantially from a truly bipartite algorithm in that they
 78 project the bipartite network into two one-mode networks (one for the higher, one for the lower
 79 level) and then proceed identifying the modules for the two levels separately, although they discuss
 80 the approach later developed by Barber (2007). The Guimerà *et al.* approach was used in several
 81 ecological applications of modularity (Olesen *et al.*, 2007; Dupont & Olesen, 2009; Fortuna *et al.*,
 82 2010; Carstensen *et al.*, 2011; Trøjelsgaard & Olesen, 2013), although the algorithm does not
 83 allow for the identification of combined modules (as stated in Barber, 2007; Fortuna *et al.*, 2010).
 84 Most recently, Thébault (2013) investigated, through simulations, the ability of three modularity
 85 measures (those of Newman & Girvan, 2004; Guimerà *et al.*, 2007; Barber, 2007) to identify
 86 modules in binary bipartite networks and comes out in support of that of Guimerà *et al.* (2007).

87 Finally, Allesina & Pascual (2009) have proposed an approach for one-mode networks. It
 88 identifies “groups”, rather than modules, which reveal more about the structure of a food web
 89 than modules do, since also their relation towards each other emerges from the analysis. Their
 90 approach is based on a binary one-mode matrix, however, even when applied to bipartite networks
 91 (as was done by Martín González *et al.*, 2012).

92 2.1 QuaBiMo: a Quantitative Bipartite Modularity algorithm

93 2.1.1 Outline

94 The new algorithm builds on the Hierarchical Random Graph approach of Clauset *et al.* (2008),
 95 which builds a graph (i.e. a dendrogram) of interacting species so that nearby species are more
 96 likely to interact. It then randomly swaps branches at any level and evaluates whether the new

graph is more likely than the previous one, recording and updating the best graph. The swapping is a Simulated Annealing-Monte Carlo approach, i.e. sometimes a worse graph is chosen as the starting point for the next swap, thereby avoiding being trapped in a local maximum. Each node of the graph contains the information of whether it is part of a module, so that the graph can be transgressed top-down to identify modules.

Our modifications consists of (a) allowing branches between species to be weighted by the number of interactions observed between them, thereby making the algorithm quantitative; and (b) taking into account that species in one group can only interact with species in the other group, rather than the one-mode network the algorithm was initially developed for. Taken together, our algorithm computes modules in weighted, bipartite networks, based on a hierarchical representation of species link weights and optimal allocation to modules.

2.1.2 Terminology

A graph $G = (V, E)$ denotes a set of vertices $v \in V$ connected by edges $e \in E$. An edge e connects two nodes, thus $e = c(v_i, v_j)$, where $v_i \in V \wedge v_j \in V$. G is a weighted (= quantitative) graph if each edge e has a weight $w \in W$ associated with it ($w \subseteq \mathbb{R}^+$). We normalise edge weights so that $\sum_{w \in W} w = 1$. (For binary graphs $w = 1/|E|$ for all existing edges, where $|\cdot|$ symbolises the number of elements.)

For bipartite graphs, the vertices V are of two non-overlapping subsets, V_H and V_L (higher and lower level), such that $V_H \cap V_L = \emptyset$ and for all edges the connected vertices are in different subsets: $v_i \in V_H \iff v_j \in V_L$ (\iff symbolises equivalence, i.e. if we know v_i is in V_H , v_j must be in V_L , and vice versa).

A graph can be represented as a dendrogram D , i.e. a binary tree with the vertices of the graph G being the tips (or leaves) of the dendrogram D . Thus, any internal split (or vertex) of D defines a subset of G . The idea of the algorithm is now to find internal vertices of D so that the subset it defines is a module.

2.1.3 Goal function

The algorithm has to divide G into a set of modules M such that

1. each module $m \in M$ is a connected subgraph of G . (This means each species has to have a partner.)
2. each vertex v belongs to exactly one module m . (The uniqueness requirement.)
3. edge weights within a module are higher than edge weights outside modules. (The modularity definition.)

To specify point 3 above, Barber (2007) has defined modularity for weighted bipartite networks as

$$Q = \frac{1}{2N} \sum_{ij} (A_{ij} - K_{ij}) \delta(m_i, m_j) \quad (1)$$

where N is the total number of observed interactions in the network and A_{ij} is the normalised observed number of interactions between i and j , i.e. the edge matrix \mathbf{E} . The expected value, based on an appropriate null model, is given in the matrix \mathbf{K} (see below). (Without normalisation, \mathbf{A} and \mathbf{K} represent the adjacency matrix and the null model matrix, respectively.) The module to which a species i or j is assigned is m_i, m_j . The indicator function $\delta(m_i, m_j) = 1$ if $m_i = m_j$ and 0 if $m_i \neq m_j$. Q ranges from 0, which means the community has no more links within modules than expected by chance, to a maximum value of 1. The higher Q , the more do the data support the division of a network into modules.

One crucial point of our modifications of the original algorithm was to assign an indicator value to each dendrogram vertex to label it as being within a module, or not. To do so, we have to compute the expected value for each value of A_{ij} in order to be able to evaluate whether the observed value is lower or higher (the term over which eqn. 1 sums). This step is not required

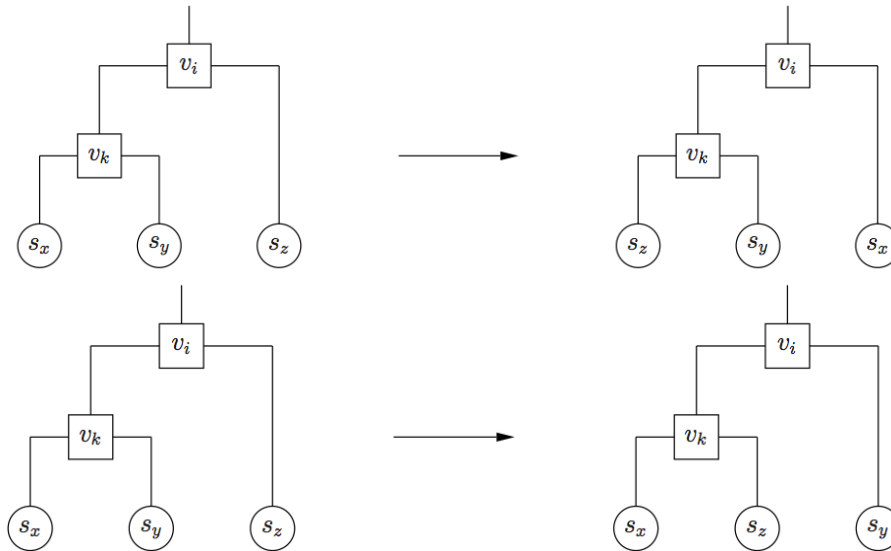


Figure 3: Two possible moves in the swapping of randomly selected vertices v_i and v_k . The leaves depicted here could be actual leaves or, more often, sub-tree and are hence labelled s . The algorithm randomly chooses one of these two possible new configurations.

143 if edges are unweighted, since then the expectation will always be the same. For weighted edges
 144 however, we would expect the edge e_{ij} connecting two nodes i and j representing abundant species
 145 to have a high value of w_{ij} . Similarly, nodes representing rare species could be expected to have
 146 low edge weights.

147 Thus, at every vertex of the tree, the algorithm assembles the module defined by the vertex'
 148 position (i.e. including all leaves on its branches) and computes the expectation matrix \mathbf{K} based
 149 on the cross product of marginal totals of all species in the module $\mathbf{A}_{.j}$ and $\mathbf{A}_{i.}$, divided by the sum
 150 of the number of observed interactions in that module: $\mathbf{K} = \mathbf{A}_{.j}^T \mathbf{A}_{i.}$. Since we normalised all edge
 151 weight to sum to 1, \mathbf{K} is actually a probability matrix. If the vertex gives rise to a module, i.e. if
 152 $\sum_{ij \in m} (A_{ij} - K_{ij}) > 0$, this vertex is labelled as a module. We can now sum the contributions of all
 153 vertices and modules according to eqn. 1 to compute to total modularity of graph G . For a formal
 154 description of this part of the algorithm, please see appendix A.

155 2.1.4 Swapping

156 The algorithm starts with a random dendrogram, where modularity Q is likely to be very low.
 157 Through random swapping of branches and their optimisation, Q increases during a Simulated
 158 Annealing procedure. The algorithm stops when a pre-defined number of swaps did not further
 159 increase the value of Q .

160 Random swaps are implemented as exchange of two randomly selected vertices in the dendro-
 161 gram, subject to the following constraint (Fig. 3). The vertex to be swapped cannot be a leaf. Since
 162 terminal vertices always connect leaves from the two bipartitions V_i and V_j , thus representing an
 163 interaction, they can be swapped, while their leaves cannot.

164 After each swap, the modularity of the entire dendrogram is re-computed (for computational
 165 efficiency only those parts affected by the swap). If the new configuration has a higher value of Q
 166 it is stored and becomes the new best dendrogram, otherwise the previous configuration will be
 167 used as the starting point for the next swap. A worse configuration is accepted with the probability
 168 $p < e^{\frac{\delta Q}{T}}$, where δQ is the change in modularity from the last configuration to the new one and T
 169 is the current temperature of the Simulated Annealing algorithm. We observed that the algorithm
 170 converges notably faster if the temperature is not decreased monotonously, but rather set back to
 171 the average temperature at which an increase in Q occurs. This is also a better approach in our
 172 case, since we do not know, a priori, how many steps the algorithm will take, or which value of Q

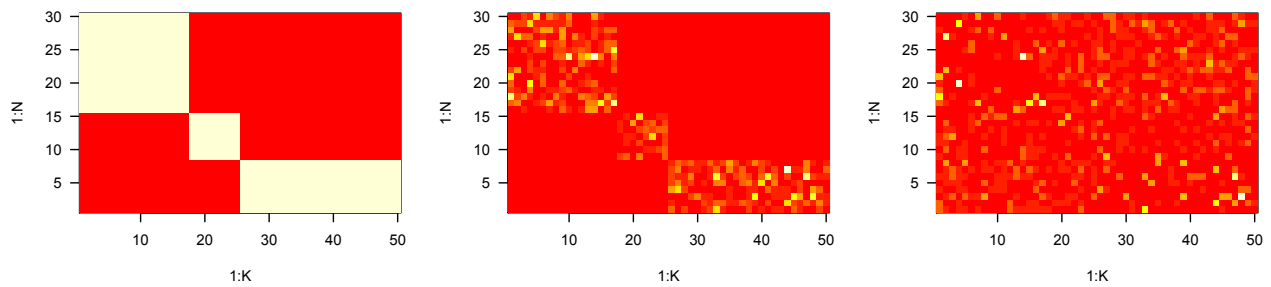


Figure 4: Network simulation starts by defining the modules (left), then allocating to all links a number of interactions drawn from a negative binomial distribution (centre) and finally removing interactions in a module and placing them outside (right). High levels of noise, as shown here, yield poorly defined modules. Cells with a value of 0 are shown in red.

173 can be obtained.

174 Since the hierarchical dendrogram is computed through iterative proposing, evaluation and
 175 rejecting dendrogram structure in a Markov Chain Monte Carlo approach, Clauset *et al.* (2008)'s,
 176 and hence our, algorithm cannot guarantee finding the optimal module configuration. Since the
 177 algorithm is coded in C++, even billions of MCMC swaps are feasible in a few minutes, yielding
 178 reasonable results for typically sized ecological networks (see below) at acceptable handling time.
 179 For large networks, this algorithm can run for hours to days. See section 5 for an example session
 180 on how to employ the algorithm through R (R Development Core Team, 2012).

181 2.2 Output & nested modules

182 The algorithm returns an object identifying modules and sequence-vectors for species, as well as
 183 a re-order network ready for visualisation of modules and the modularity Q .

184 QuaBiMo can be invoked recursively, searching for modules within modules. While such
 185 nested modules become ever smaller and are thus ever faster to detect, there are plenty of them
 186 and hence nesting will typically dramatically prolong the search for patterns.

187 3 Evaluation of the algorithm

188 The detection of modules has theoretical limits related to the number of between-module links
 189 present, the sparceness of the network matrix and the size of the network (e.g. Fortunato &
 190 Barthélemy, 2007; Lancichinetti & Fortunato, 2011; Lancichinetti *et al.*, 2010). In the follow-
 191 ing paragraphs we evaluate the QuaBiMo-algorithm for different simulated networks typical in
 192 size and noise for pollination networks. There is no technical reason why the algorithm should
 193 not work for much larger networks, too, given enough time for computing a large number of
 194 dendrogram configurations. Such an evaluation is outside the scope of this study.

195 3.1 Simulations to investigate algorithm sensitivity and specificity 196 for noisy network data

197 We analysed simulated networks of different noisiness to evaluate the performance of the mod-
 198 ularity algorithm. We would expect that modules become unidentifiable when the proportion of
 199 links within modules becomes as low as between modules. We hence simulate networks with in-
 200 creasing degree of noise by moving, randomly, interactions from within a module to a random
 201 position in the adjacency matrix not included in any module (Fig. 4). We simulated two sizes of
 202 networks (30×50 and 100×400), two levels of filling (achieved through setting the parameter

203 “size” of the negative binomial distribution to 0.1, “low”, or 1, “high”), and two levels of mod-
204 ularisation (3 and 10 modules). Each combination was evaluated for seven noise levels (0, 0.05,
205 0.1, 0.2, 0.3, 0.4, 0.5) and replicated 15 times, yielding 840 different networks. Replicates differ
206 in the size, position of modules and number of interactions per link. Sizes were maintained at the
207 same two levels.

208 Networks were simulated in three steps. First, we defined the size of the matrix and position
209 and size of the modules. This initial network is a matrix of 0s except for all interactions in a
210 module, which is thus identified by a block of 1s. Then, second, we drew actual interactions for
211 each link of a module from a strongly skewed negative binomial distribution (with size = 0.05 and
212 $\mu = 2$), removed 80% (high filling) or 40% (low filling) of 0-values, and then replaced the initial
213 1s of the module blocks by these random values. Accordingly, the modules had a connectance (=
214 filling) of less than 100%. Higher filling of modules generally increases performance. Third, we
215 randomly drew a proportion of interactions from the module and moved it to randomly selected
216 columns and rows of these species outside the module. Thereby we effectively added noise to the
217 network data. There is an upper limit to the third step, where modules become ill-defined. That is
218 the case when the number of interactions outside modules is as high as inside.

219 We ran the QuaBiMo algorithm five times on each network, saving the result with the highest
220 modularity. This was more efficient in finding a good module configuration than running the
221 algorithm for much longer. For comparison, we also ran the algorithm on a binarised version
222 of the data. The code for simulations and analysis is available in appendix B; runtime for the
223 simulations was approximately two weeks on a standard desktop computer with 32 GB RAM.

224 Congruence between the original assignment to modules and the one identified by the algo-
225 rithm was assessed by means of a confusion matrix. Each link existing in the simulated data was
226 classified as correctly belonging to a module, falsely assigned to a module, falsely not assigned to
227 a module, or correctly not assigned to a module. The confusion matrix was then summarised as
228 sensitivity, specificity and accuracy.

229 **3.2 Simulation results: modularity Q in binary and weighted net-** 230 **works**

231 Modularity Q was strongly dependent on network size, the amount of noise added and the number
232 of modules (Table 1). Most importantly, however, our quantitative approach strongly improved
233 on modularity based on binary data, particularly for large networks (Fig. 5). Deterioration of the
234 module detection with increasing network size could possibly be compensated for by increasing
235 the number of swaps before terminating the search (see example session below). The loss of skill
236 with increasing noise (Fig. 5, right) cannot be alleviated. Here the ability of QuaBiMo to use not
237 only the binary but the weighted link information is already a dramatic improvement.

238 In the following paragraphs, we shall only be looking at the results for the weighted networks,
239 since that is the explicit focus of the QuaBiMo algorithm.

240 **3.3 Simulation results: modularity Q**

241 Modularity Q and overall accuracy were affected very similarly by network size, noise and the
242 number of modules (Table 2). The most prominent effects were those of size, noise and their
243 interaction, depicted for Q and overall accuracy in Fig. 6. Evidently, larger networks are more
244 difficult to modularise, as are those with a higher level of noise.

245 **3.4 Simulation results: classification accuracy**

246 While modularity Q gives an indication of how well observed links could be grouped into mod-
247 ules (with a value of 1 indicating that all links are within and none between modules), we can also
248 quantify the algorithm’s accuracy based on a confusion table. Overall accuracy (= correct classi-
249 fication rate) is the proportion of all links correctly placed, i.e. (number of links correctly placed

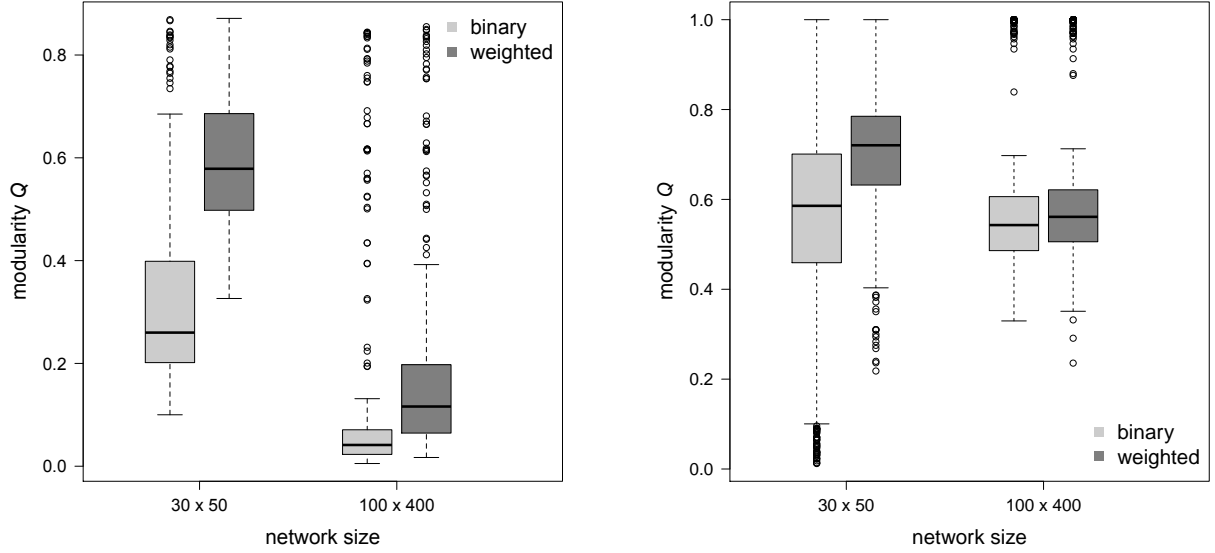


Figure 5: Quality of modularity detection (left: Q ; right: overall accuracy) depends on network size and type of information (binary or weighted).

Table 1: Effect of different simulation parameters on modularity Q and overall accuracy. Sum of squares and F -value can be taken as a measure of how strongly these parameters effect modularity. No significances are given since a test of an effect is nonsensical for simulations. Information refers to binary vs. weighted networks. ‘Noise’ has seven levels but was analysed as continuous variable.

Modularity Q	df	sum of squares	F value
noise	1	17.78	1024
size	1	38.24	2204
fill	1	1.06	61
no.of.modules	1	6.02	346
information	1	11.65	671
noise:size	1	0.30	18
noise:no.of.modules	1	2.01	116
size:fill	1	0.57	33
size:no.of.modules	1	0.42	24
size:information	1	4,27	246
Residuals	1635	28.37	
Overall accuracy	df	sum of squares	F value
noise	1	7.59	296
size	1	0.24	9
fill	1	0.74	29
no.of.modules	1	2.30	90
information	1	2.60	102
noise:size	1	0.35	14
noise:fill	1	0.62	24
noise:no.of.modules	1	0.46	18
noise:information	1	2.33	91
size:fill	1	0.24	9
size:no.of.modules	1	1.32	52
size:information	1	1.81	71
no.of.modules:information	1	0.87	34
Residuals	1632	41.86	

Table 2: Effect of different simulation parameters on modularity Q for weighted networks. Sum of squares and F -value can be taken as a measure of how strongly these parameters effect modularity.

	df	sum of squares	F value
noise	1	7.56	584
size	1	33.64	2597
fill	1	0.59	45
no.of.modules	1	3.76	290
noise:size	1	0.40	31
noise:no.of.modules	1	0.55	43
size:fill	1	0.23	18
size:no.of.modules	1	0.12	9
Residuals	809	10.48	

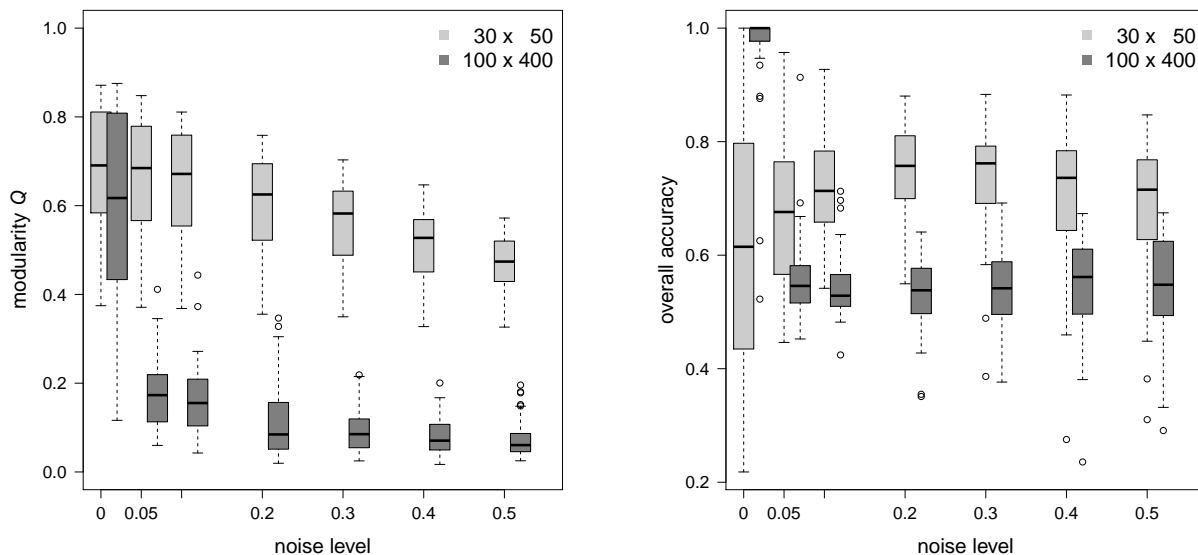


Figure 6: Effect of noise and network size on modularity Q (left) and overall accuracy (left).

Table 3: Effect of different simulation parameters on module identification accuracy (weighted networks only).

	df	sum of squares	F value
noise	1	0.74	41
size	1	1.65	90
fill	1	0.84	46
no.of.modules	1	0.18	10
noise:size	1	1.95	106
noise:fill	1	0.14	8
noise:no.of.modules	1	0.11	6
size:fill	1	0.32	17
size:no.of.modules	1	0.17	9
Residuals	808	14.80	

into modules + number of links correctly placed between modules)/total number of links. Since the purpose of the algorithm is the use of weighted network data, we here only present results for the weighted and not for the binary networks.

The overall accuracy of module detection decreased with increasing noise levels (Table 3), an effect more pronounced for large networks than for small ones (Fig. 6 right). Again, this interaction probably could have been reduced if more steps until termination were allowed for the larger networks.

3.5 Simulation results: sensitivity and specificity

Classification accuracy has two elements: the correct classification of all module links as belonging to modules (sensitivity) and the correct identification of between-module links as *not* belonging into modules (specificity). For the detection of patterns in networks high sensitivity is desirable, although this may inflate type II errors (i.e. we may identify modules that do not really exist). High specificity indicates that links allocated into modules are indeed correct, but possibly at the expense of not allocating many links to modules overall (leading to inflated type I errors).

Sensitivity and specificity of the QuaBiMo-algorithm were driven by the same factors as overall accuracy (Table 4). Increasing noise levels reduced both sensitivity and specificity, as did larger networks (Fig. 7).

4 Identifying modules - an example session

The QuaBiMo-algorithm is implemented in C++ and is made available through the open source R-package `bipartite` (Dormann *et al.*, 2009). The most important function is `computeModules`, which takes three arguments: the matrix representing the bipartite network data (“web”), a specification of how many MCMC moves should yield no improvement before the algorithm stops (“steps”, with default $1E6$) and a logical switch for computing nested modules (“deep”, defaulting to `FALSE`). The number of steps should be adapted to the size of the network (see previous sections). We found that Q levels off very soon, once the default of one million is exceeded. However, we have not extensively trialled this setting for networks larger than that used below.

As a typical analysis we shall use the relatively large (25×79) and well-sampled pollination network of Memmott (1999), which is provided along with the `bipartite` package:

```
> library(bipartite)
> mod <- computeModules(web=memmott1999, steps=1E8)
```

The evaluation of these two lines will usually take about one minute and perform around 20 million MCMC moves. The resulting object stores the module composition and the likelihood of

Table 4: Effect of different simulation parameters on sensitivity and specificity of module identification (weighted networks only).

Sensitivity	df	sum of squares	<i>F</i> -value
noise	1	8.48	278
size	1	3.34	109
fill	1	0.46	15
no.of.modules	1	3.01	99
noise:size	1	0.27	9
noise:fill	1	0.65	21
size:fill	1	0.81	27
Residuals	810	24.75	
Specificity	df	sum of squares	<i>F</i> -value
noise	1	5.84	308
size	1	11.73	618
fill	1	0.48	25
no.of.modules	1	0.24	13
Residuals	813	15.44	

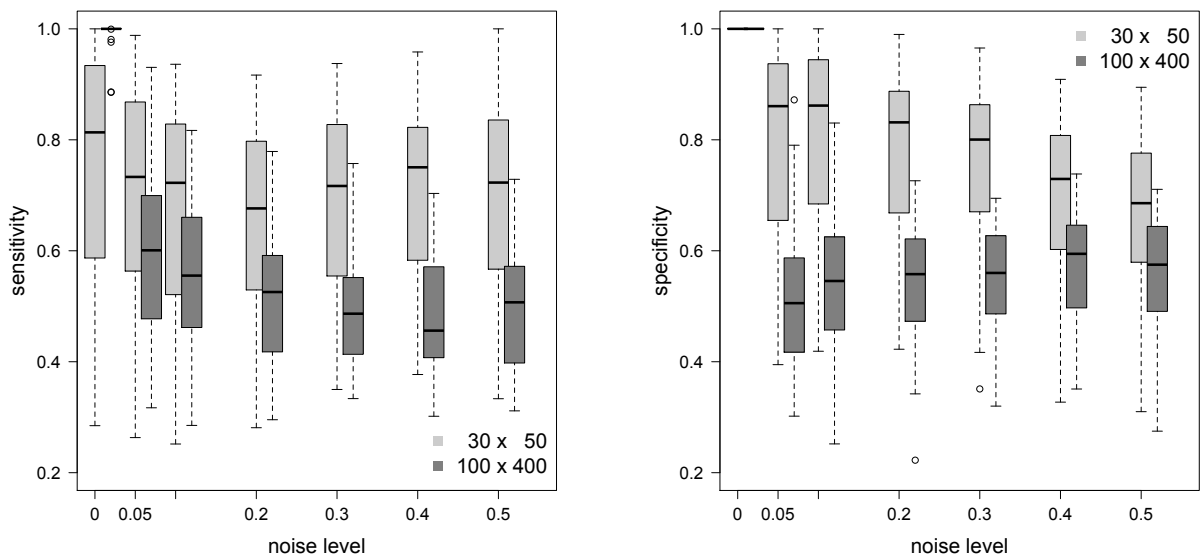


Figure 7: Effect of noise and network size on sensitivity (right) and specificity (left) of the classification of links into modules.

282 the solution found. The modularity value Q of this solution is simply the likelihood value (0.18,
283 this value may vary between runs; random seeding is not supported):

```
284 > mod@likelihood  
285 [1] 0.18
```

286 We can now plot the resulting modules to visualise the compartments (Fig. 8 top).

```
287 > plotModuleWeb(mod)
```

288 To identify nested modules, we choose a lower value for steps (to reduce computation time), thus
289 also yielding a different module structure at the highest level. Modularity value Q will still be
290 based on the non-recursive algorithm.

```
291 > modn <- computeModules(memmott1999, steps=1E6, deep=T)
```

292 To be able to ecologically interpret these modules (Fig. 8 bottom), expert knowledge on the system
293 is required. The computation of modularity is primarily an explorative tool helping the user to
294 objectively detect pattern in typically noisy network data.

295 5 Modularity Q as a network index

296 Modularity Q is likely to be correlated with other network metric, as specialisation of module
297 members is the prime reason for the existence of modules. Across the 22 quantitative pollina-
298 tion networks of the NCEAS “interaction webs” data base ([http://www.nceas.ucsb.edu/](http://www.nceas.ucsb.edu/interactionweb)
299 [interactionweb](http://www.nceas.ucsb.edu/interactionweb)), Q was evidently highly positively correlated with complementary speciali-
300 sation H'_2 (Fig. 9). Ecologically, the correlation with specialisation makes good sense. Modules
301 only exist because some species do not interact with some others, i.e. because they are specialised.
302 An overall low degree of specialisation is equivalent to random interactions, which will yield no
303 modules.

304 Furthermore, the absolute value of Q (like all network indices: Dormann *et al.*, 2009) is de-
305 pendent on network size (i.e. the number of species) as well as the number of links and the total
306 number of interactions observed (see also Thébault, 2013). We would thus recommend a null
307 model comparison (e.g. Vázquez & Aizen, 2003; Blüthgen *et al.*, 2008; Dormann *et al.*, 2009) to
308 correct the observed value of Q by null model expectation (e.g. by standardising them to z -scores:
309 $z_Q = \frac{Q_{\text{observed}} - \bar{Q}_{\text{null}}}{\sigma_{Q_{\text{null}}}}$). In R, this could be achieved by the following code (which will take more than
310 one hour since we are computing modules in 100 null model networks):

```
311 > nulls <- nullmodel(memmott1999, N=100, method="r2d")  
312 > modules.nulls <- sapply(nulls, computeModules)  
313 > like.nulls <- sapply(modules.nulls, function(x) x@likelihood)  
314 > (z <- (mod@likelihood - mean(like.nulls))/sd(like.nulls))  
315  
316 [1] 7.088665
```

317 This means that the observed modularity is 7 standard deviations higher than would be expected
318 from random networks with the same marginal totals (representing abundance distributions of
319 plants and pollinators). Since z -scores are assumed to be normally distributed, values above ≈ 2
320 are considered significantly modular.

321 5.1 Using modularity to identifying species with important roles in 322 the network

323 Guimerà *et al.* (2005) and Olesen *et al.* (2007) propose to compute standardised connection and
324 participation values, called c and z , for each species to describe their role in networks, where

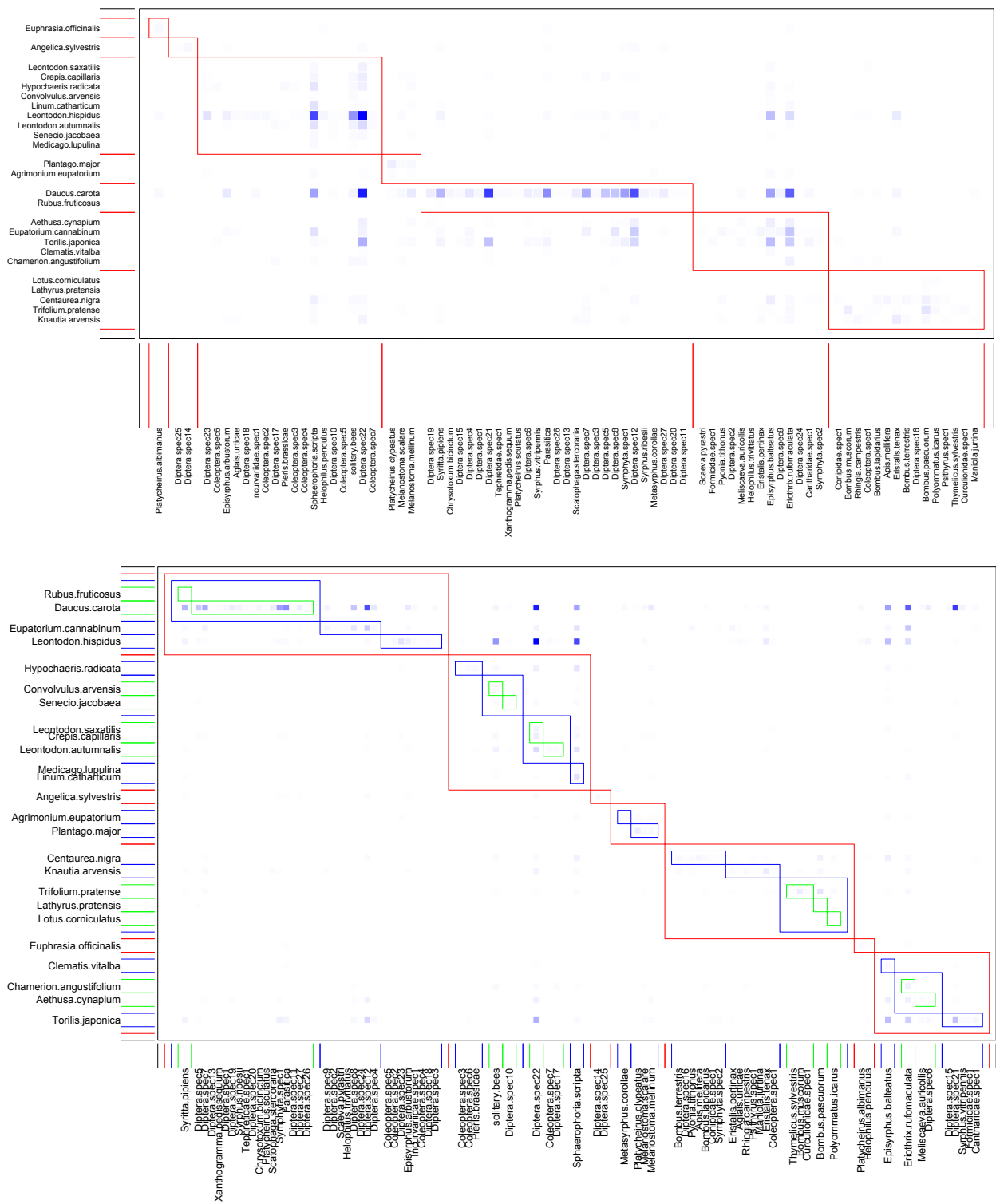


Figure 8: Interaction matrix featuring modules for the data of Memmott (1999). *Top*: Modules identified by QuaBiMo (with steps=1E10, running for several hours; $Q = 0.30$). Darker squares indicate more observed interactions. Red boxes delineate the seven modules. (Note that results may vary between runs.) In the central module yellow Asteraceae feature heavily, while a possible ecological cause pattern for the other modules is less apparent. *Bottom*: Nested modules based on a recursive call of QuaBiMo. Module arrangement is slightly different from top, since the algorithm is stochastic.

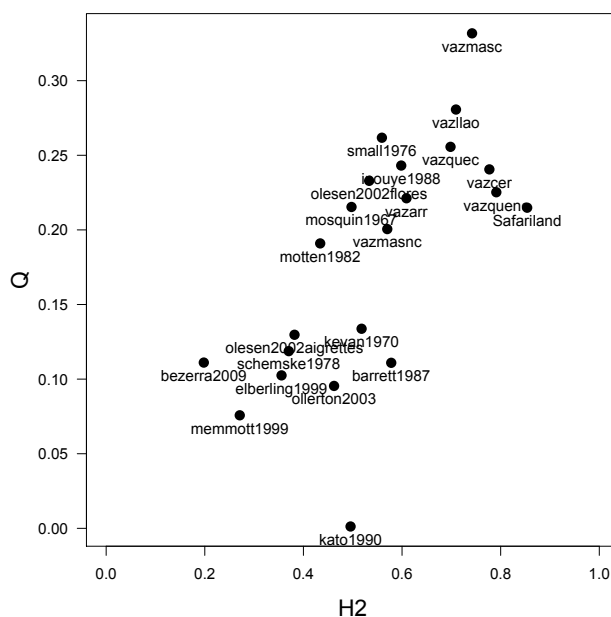


Figure 9: Modularity (Q) is highly correlated with specialisation H_2^l (Blüthgen *et al.*, 2006) across 22 pollination networks. Names refer to network data sets in bipartite which were taken from <http://www.nceas.ucsb.edu/interactionweb>.

325 c refers to the between-modules connectivity (called “participation coefficient” P by Guimerà
 326 *et al.*, 2005) and z refers to within-module degrees. Both are computed on the number of links
 327 and are not weighted by the number of interactions per link. Guimerà *et al.* (2005) suggest critical
 328 values of c and z of 0.625 and 2.5, respectively. Species exceeding both of these values are called
 329 “hubs” because they link different modules, combining high between- with high within-module
 330 connectivity.

331 In the case of the pollination network of Fig. 1, c -values range between 0 and 0.78 (with 23
 332 of 79 pollinators and 13 of 25 plant species exceeding the threshold of 0.625); z -values range
 333 between -1.21 and 5.00 (with two pollinators but no plant species exceeding the value of 2.5;
 334 Fig. 10). Put together, only the syrphid *Syrirta pipiens* (and hawkbit *Leontodon hispidus* almost)
 335 exceeded both thresholds and would thus be called a “hub species”. As can be seen in Fig. 8, this
 336 syrphid is relatively rare but clearly not randomly distributed over the six modules, thus linking
 337 modules three, five and six (from the left). In contrast, *Leontodon hispidus* is a common plant
 338 species, visited by many different pollinators, and it actually links all modules with the exception
 339 of module two.

340 To objectively define this threshold one could run null models of the original network and
 341 employ 95% quantiles as critical c - and z -values. For the pollinators in the network of Fig. 1
 342 these would be $0.67 (\pm 0.039)$ and $1.45 (\pm 0.220)$, respectively, based on 100 null models (for
 343 the plants: $c_{\text{critical}} = 0.72 \pm 0.036$ and $z_{\text{critical}} = 1.78 \pm 0.297$; Fig. 10 left). While this has little
 344 effect for plant species (except for moving *Leontodon hispidus* across the threshold), three more
 345 pollinators would become hub species (the common hoverfly *Episyrphus balteatus*, the tachinid
 346 fly *Eriothrix rufomaculata* and undetermined fly “*Diptera spec.22*”).

347 6 Conclusion

348 We here presented an algorithm to compute modularity Q and detect modules in weighted, bipar-
 349 tite networks. In a preliminary analysis, this approach was able to identify meaningful ecological
 350 modules in frugivore networks (Schleuning *et al.*, in submission). Because it uses the strength
 351 of links as quantitative information, this approach should be much more sensitive, and also more

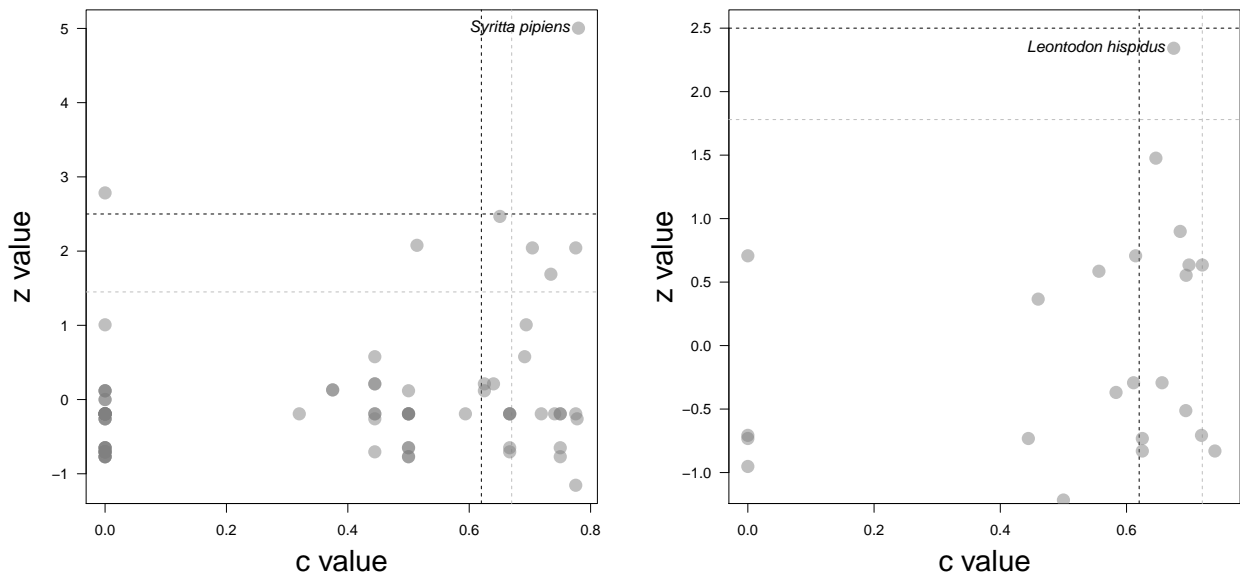


Figure 10: Connection (c) and participation (z) values for pollinators (left) and plants (right) in the network of Memmott (1999). Dashed black lines indicate critical values according to Olesen *et al.* (2007), those in grey 95% quantiles from 100 null models (see text).

352 specific, than current binary algorithms. By making the algorithm easily available we hope that
 353 network ecology will benefit from new insights into the structure of interaction networks.

354 7 Acknowledgements

355 We like to thank Aaron Clauset for inventing the hierarchical random graph idea and for making
 356 his code freely available. CFD acknowledges funding by the Helmholtz Association (VH-NG
 357 247). Many thanks to Lili Ingmann and Matthias Schleuning for extensively testing the robustness
 358 and ecological meaningfulness of this algorithm.

359 References

- 360 Allesina, S. (2009) Cycling and cycling indices. S.E. Jorgensen, ed., *Ecosystem Ecology*, pp.
 361 50–57. Elsevier, Amsterdam.
- 362 Allesina, S. & Pascual, M. (2009) Food web models: a plea for groups. *Ecology Letters*, **12**,
 363 652–62.
- 364 Barber, M. (2007) Modularity and community detection in bipartite networks. *Physical Review*
 365 *E*, **76**, 1–9.
- 366 Bascompte, J., Jordano, P., Melián, C.J. & Olesen, J.M. (2003) The nested assembly of
 367 plant–animal mutualistic networks. *Proceedings of the National Academy of Sciences of the*
 368 *USA*, **100**, 9383–9387.
- 369 Blüthgen, N. (2010) Why network analysis is often disconnected from community ecology: A
 370 critique and an ecologist’s guide. *Basic and Applied Ecology*, **11**, 185–195.
- 371 Blüthgen, N., Fründ, J., Vázquez, D.P. & Menzel, F. (2008) What do interaction network metrics
 372 tell us about specialization and biological traits? *Ecology*, **89**, 3387–99.

- 373 Blüthgen, N., Menzel, F. & Blüthgen, N. (2006) Measuring specialization in species interaction
374 networks. *BMC Ecology*, **6**, 9.
- 375 Borgatti, S.P. (2006) Identifying sets of key players in a social network. *Computational and*
376 *Mathematical Organization Theory*, **12**, 21–34.
- 377 Cagnolo, L., Salvo, A. & Valladares, G. (2010) Network topology: patterns and mechanisms in
378 plant-herbivore and host-parasitoid food webs. *Journal of Animal Ecology*, pp. 342–351.
- 379 Carstensen, D.W., Dalsgaard, B., Svenning, J.C., Rahbek, C., Fjeldså, J., Sutherland, W.J. & Ole-
380 sen, J.M. (2011) Biogeographical modules and island roles: a comparison of wallacea and the
381 west indies. *Journal of Biogeography*, **39**, 739–749.
- 382 Clauset, A., Moore, C. & Newman, M.E.J. (2008) Hierarchical structure and the prediction of
383 missing links in networks. *Nature*, **453**, 98–101.
- 384 Clauset, A., Newman, M. & Moore, C. (2004) Finding community structure in very large net-
385 works. *Physical Review E*, **70**, 066111.
- 386 Danieli-Silva, A., de Souza, J.M.T., Donatti, A.J., Campos, R.P., Vicente-Silva, J., Freitas, L. &
387 Varassin, I.G. (2011) Do pollination syndromes cause modularity and predict interactions in a
388 pollination network in tropical high-altitude grasslands? *Oikos*, **121**, 35–43.
- 389 Dicks, L.V., Corbet, S.A. & Pywell, R.F. (2002) Compartmentalization in plant–insect flower
390 visitor webs. *Journal of Animal Ecology*, **71**, 32–43.
- 391 Dormann, C.F., Blüthgen, N., Fründ, J. & Gruber, B. (2009) Indices, graphs and null models:
392 Analyzing bipartite ecological networks. *The Open Ecology Journal*, **2**, 7–24.
- 393 Dupont, Y.L. & Olesen, J.M. (2009) Ecological modules and roles of species in heathland plant:
394 insect flower visitor networks. *Journal of Animal Ecology*, **78**, 346–353. 10.1111/j.1365-
395 2656.2008.01501.x.
- 396 Fortuna, M.A., Stouffer, D.B., Olesen, J.M., Jordano, P., Mouillot, D., Krasnov, B.R., Poulin, R.
397 & Bascompte, J. (2010) Nestedness versus modularity in ecological networks: two sides of the
398 same coin? *Journal of Animal Ecology*, **79**, 811–7.
- 399 Fortunato, S. (2010) Community detection in graphs. *Physics Reports*, **486**, 75–174.
- 400 Fortunato, S. & Barthélemy, M. (2007) Resolution limit in community detection. *Proceedings of*
401 *the National Academy of Sciences of the USA*, **104**, 36–41.
- 402 Garcia-Domingo, J.L. & Saldaña, J. (2008) Effects of heterogeneous interaction strengths on food
403 web complexity. *Oikos*, **117**, 333–343.
- 404 Guimarães Jr, P.R., Jordano, P. & Thompson, J.N. (2011) Evolution and coevolution in mutualistic
405 networks. *Ecology Letters*, **14**, 877–885.
- 406 Guimerà, R., Mossa, S., Turtschi, A. & Amaral, L.A.N. (2005) The worldwide air transportation
407 network: Anomalous centrality, community structure, and cities' global roles. *Proceedings of*
408 *the National Academy of Sciences of the USA*, **102**, 7794–9.
- 409 Guimerà, R., Sales-Pardo, M. & Amaral, L. (2007) Module identification in bipartite and directed
410 networks. *Physical Review E*, **76**, 036102.
- 411 Ings, T.C., Montoya, J.M., Bascompte, J., Blüthgen, N., Brown, L., Dormann, C.F., Edwards, F.,
412 Figueroa, D., Jacob, U., Jones, J.I., Lauridsen, R.B., Ledger, M.E., Lewis, H.M., Olesen, J.M.,
413 van Veen, F.J.F., Warren, P.H. & Woodward, G. (2009) Ecological networks—beyond food webs.
414 *Journal of Animal Ecology*, **78**, 253–69.

- 415 Jacobi, M.N., André, C., Döös, K. & Jonsson, P.R. (2012) Identification of subpopulations from
416 connectivity matrices. *Ecography*, **35**, 1004–1016.
- 417 Joppa, L.N., Bascompte, J., Montoya, J.M., Solé, R.V., Sanderson, J. & Pimm, S.L. (2009) Recip-
418 rocal specialization in ecological networks. *Ecology Letters*, **12**, 961–969.
- 419 Lancichinetti, A. & Fortunato, S. (2011) Limits of modularity maximization in community detec-
420 tion. *Physical Review E*, **84**, 066122.
- 421 Lancichinetti, A., Kivela, M., Saramaki, J. & Fortunato, S. (2010) Characterizing the community
422 structure of complex networks. *PLoS ONE*, **5**, e11976.
- 423 Levins, R. (1975) Evolution in communities near equilibrium. M.L. Cody & J.M. Diamond, eds.,
424 *Ecology and Evolution of Communities*, pp. 16–50. Belknap Press, Cambridge, MA.
- 425 Lewinsohn, T.M., Prado, P.I., Jordano, P., Bascompte, J. & Olesen, J.M. (2006) Structure in plant-
426 animal interaction assemblages. *Oikos*, **113**, 174–184.
- 427 Martín González, A.M., Allesina, S., Rodrigo, A. & Bosch, J. (2012) Drivers of compartmental-
428 ization in a mediterranean pollination network. *Oikos*, **121**, 2001–2013.
- 429 May, R.M. (1973) *Stability and Complexity in Model Ecosystems*. Princeton University Press,
430 Princeton.
- 431 Memmott, J. (1999) The structure of a plant-pollinator food web. *Ecology Letters*, **2**, 276–280.
- 432 Morris, R.J., Lewis, O.T. & Godfray, H.C.J. (2004) Experimental evidence for apparent competi-
433 tion in a tropical forest food web. *Nature*, **428**, 310–313.
- 434 Newman, M.E.J. (2003) The structure and function of complex networks. *SIAM Review*, **45**,
435 167–256.
- 436 Newman, M.E.J. (2004) Fast algorithm for detecting community structure in networks. *Physical*
437 *Reviews E*, **69**, 066133.
- 438 Newman, M.E.J. (2006) Modularity and community structure in networks. *Proceedings of the*
439 *National Academy of Sciences of the USA*, **103**, 8577–82.
- 440 Newman, M.E.J. & Girvan, M. (2004) Finding and evaluating community structure in networks.
441 *Physical Review E*, **69**, 1–15.
- 442 Olesen, J.M., Bascompte, J., Dupont, Y.L. & Jordano, P. (2007) The modularity of pollination
443 networks. *Proceedings of the National Academy of Sciences of the USA*, **104**, 19891–19896.
- 444 Pimm, S.L. (1982) *Food Webs*. Chicago University Press, Chicago.
- 445 Pocock, M.J.O., Evans, D.M. & Memmott, J. (2012) The robustness and restoration of a network
446 of ecological networks. *Science*, **335**, 973–977.
- 447 Poisot, T., Canard, E., Mouquet, N. & Hochberg, M.E. (2012) A comparative study of ecological
448 specialization estimators. *Methods in Ecology and Evolution*, **3**, 537–544.
- 449 Prado, P.I. & Lewinsohn, T.M. (2004) Compartments in insect–plant associations and their con-
450 sequences for community structure. *Journal of Animal Ecology*, **73**, 1168–1178.
- 451 R Development Core Team (2012) *R: A Language and Environment for Statistical Computing*. R
452 Foundation for Statistical Computing, Vienna, Austria.

- 453 Schleuning, M., Fründ, J., Klein, A.M., Abrahamczyk, S., Alarcón, R., Albrecht, M., Anders-
454 son, G.K.S., Bazarian, S., Böhning-Gaese, K., Bommarco, R. & et al. (2012) Specialization of
455 mutualistic interaction networks decreases toward tropical latitudes. *Current Biology*, **22**, 1–7.
- 456 Schuetz, P. & Cafilisch, A. (2008) Efficient modularity optimization by multistep greedy algorithm
457 and vertex mover refinement. *Physical Reviews E*, **77**, 046112.
- 458 Scotti, M., Podani, J. & Jordan, F. (2007) Weighting, scale dependence and indirect effects in
459 ecological networks: A comparative study. *Ecological Complexity*, **4**, 148–159.
- 460 Thébault, E. (2013) Identifying compartments in presence-absence matrices and bipartite net-
461 works: insights into modularity measures. *Journal of Biogeography*, **40**, 759–768.
- 462 Trøjelsgaard, K. & Olesen, J.M. (2013) Macroecology of pollination networks. *Global Ecology*
463 *and Biogeography*, **22**, 149–162.
- 464 Tylianakis, J.M., Laliberté, E., Nielsen, A. & Bascompte, J. (2010) Conservation of species inter-
465 action networks. *Biological Conservation*, **143**, 2270–2279.
- 466 Tylianakis, J.M., Tschardtke, T. & Lewis, O.T. (2007) Habitat modification alters the structure of
467 tropical host-parasitoid food webs. *Nature*, **445**, 202–5.
- 468 Vázquez, D.P. & Aizen, M.A. (2003) Null model analyses of specialization in plant–pollinator
469 interactions. *Ecology*, **84**, 2493–2501.
- 470 Vázquez, D.P., Blüthgen, N., Cagnolo, L. & Chacoff, N.P. (2009) Uniting pattern and process in
471 plant-animal mutualistic networks: a review. *Annals of Botany*, **103**, 1445–57.

472 **Appendix A: Formal definition of the identification of mod-** 473 **ule vertices**

474 Consider an edge $(i, j) \in E$ with weight w_{ij} representing the strength of interaction between ver-
475 tices i and j . In a bipartite graph \bar{G} maintaining for each vertex its original sum of edge weights,
476 but disregarding the modular structure of G , the weight \bar{w}_{ij} of the edge between vertices i and j is
477 given by

$$\bar{w}_{ij} = \begin{cases} \sum w_{i \cdot} \times \sum w_{\cdot j}, & \text{if } i \in V_A \Leftrightarrow j \in V_B \\ 0, & \text{else.} \end{cases} \quad (2)$$

478 Therefore, the difference of edge weight and expected edge weight

$$w'_{ij} = w_{ij} - \bar{w}_{ij} \quad (3)$$

479 is positive, if within module, and negative, if outside module.

480
481 Therefore, the algorithm attempts to find the best trade-off between a maximum sum of w'
482 within modules and a minimum sum of w' outside.

483 Given a division of V into a set of non-overlapping subgraphs C , we define

$$g(C) = \begin{cases} \sum_{i \in V_A} \sum_{j \in V_B} \delta_C(i, j) \times w'_{ij} - (1 - \delta_C(i, j)) \times w'_{ij}, & \text{if } \forall c \in C: c \text{ is connected graph} \\ -\infty, & \text{else,} \end{cases} \quad (4)$$

484 where

$$\delta_C(i, j) = \begin{cases} 1, & \text{if } i \in c \wedge j \in c \wedge c \in C \\ 0, & \text{else.} \end{cases} \quad (5)$$

485 Obviously, $g(C)$ has to be maximized in order to find the best division of V into modules C . For
 486 achieving this goal, we modify the algorithm of Clauset *et al.* (2008).

487 Let D be a binary tree with arbitrarily connected internal vertices $v \in V_{\text{intern}}$ and with n leaves
 488 representing the vertices of G and initially arranged in an arbitrary order. A module c within D
 489 is defined as the set of leaves of the sub-tree rooted at an internal vertex v meeting following
 490 requirements:

- 491 I v has at least one child being a leaf.
- 492 II No ancestor of v has a child being a leaf.
- 493 III $c \cap V_A \neq \emptyset \wedge c \cap V_B \neq \emptyset$, i.e. there is at least one vertex $v_A \in V_A$ and at least one vertex $v_B \in V_B$
 494 within c .

495 Due to requirement I it is obvious that there are at most $\min(|V_A|, |V_B|)$ modules. Note that due to
 496 requirement II on each path from the root of D to a leaf there is exactly one internal vertex shaping
 497 a module. For convenience, we will use the term 'module vertex' for this kind of vertex.

498 Each internal vertex v is assigned the information r_v whether it is the root of a sub-tree of D
 499 representing a module or whether it is below or above such an internal vertex. Let $r_v = 1$ if v is
 500 above a module vertex, $r_v = 0$ if v is a module vertex itself and let $r_v = -1$ if v is below a module
 501 vertex.

502 Additionally, each internal vertex v is assigned its contribution g_v to $g(C)$

$$g_v = \begin{cases} + \sum_{i \in \mathcal{L}_v} \sum_{j \in \mathcal{R}_v} w'_{ij}, & \text{if } r_v \leq 0 \wedge \sum_{i \in \mathcal{L}_v} \sum_{j \in \mathcal{R}_v} w_{ij} > 0 \\ - \sum_{i \in \mathcal{L}_v} \sum_{j \in \mathcal{R}_v} w'_{ij}, & \text{if } r_v = 1 \\ -\infty, & \text{else,} \end{cases} \quad (6)$$

503 where \mathcal{L}_v is the set of leaves of the sub-tree rooted at the left child of v and, analogously, \mathcal{R}_v is
 504 the set of leaves of the sub-tree rooted at the right child of v .

505 For C given by the current state of D , $g(C)$ can now be rewritten as

$$g(C) = \sum_{v \in V_{\text{intern}}} g_v \quad . \quad (7)$$

506 In order to compute $\max(g(C))$, the subtrees of D have to be re-arranged. The algorithm therefore
 507 randomly selects an edge e of D connecting two internal vertices v_i and v_j . Let w.l.o.g. e be the left
 508 edge of v_j connecting it to its child v_i . Then there are three subtrees \mathcal{L}_{v_i} , \mathcal{R}_{v_i} and \mathcal{R}_{v_j} originating
 509 from v_i and v_j , respectively, and two possible rearrangements α and β (Fig. 3) of which one is
 510 chosen randomly and simulated. In re-arrangement α , sub-trees \mathcal{R}_{v_i} and \mathcal{R}_{v_j} are permuted, in
 511 rearrangement β sub-trees \mathcal{L}_{v_i} and \mathcal{R}_{v_j} . The change dg in $g(C)$ resulting from the rearrangement
 512 is computed according to r_{v_i} and r_{v_j} .